Vibrational Modes and Dynamic Heterogeneity in a Near-Equilibrium 2D Glass of Colloidal Kites

Yiwu Zong,[1] Ke Chen,[2,3] Thomas G. Mason,[4,5] and Kun Zhao[1,*]

[1]*Key Laboratory of Systems Bioengineering (Ministry of Education), School of Chemical Engineering and Technology, Tianjin University, Tianjin 300072, People's Republic of China*

[2]*Beijing National Laboratory for Condensed Matter Physics and Key Laboratory of Soft Matter Physics, Institute of Physics, Chinese Academy of Sciences, Beijing 100190, People's Republic of China*

[3]*Songshan Lake Materials Laboratory, Dongguan, Guangdong 523808, People's Republic of China*

[4]*Department of Physics and Astronomy, University of California–Los Angeles, Los Angeles, California 90095, USA*

[5]*Department of Chemistry and Biochemistry, University of California–Los Angeles, Los Angeles, California 90095, USA*

(Received 2 May 2018; revised manuscript received 4 September 2018; published 30 November 2018)

Using video microscopy and particle-tracking techniques developed for dense Brownian systems of polygons, we study the structure-dynamics relationship in a near-equilibrium 2D glass consisting of anisotropic Penrose kite-shaped colloids. Detailed vibrational properties of kite glasses, both translational and rotational, are obtained using covariance matrix techniques. Different from other colloidal glasses of spheres and ellipsoids, the vibrational modes of kite glasses at low frequencies show a strong translational character with spatially localized rotational modes and extended translational modes. Low-frequency quasilocalized soft modes commonly found in sphere glasses are absent in the translational phonon modes of kite glasses. Soft modes are observed predominantly in the rotational vibrations and correlate well with the spatial distribution of Debye-Waller factors. The local structural entropy field shows a strong correlation with the observed dynamic heterogeneity.

DOI: 10.1103/PhysRevLett.121.228003

Introduction.—The exact nature of glassy materials and the glass transition is a long-standing unsolved problem in condensed matter physics [1]. In glass-forming molecular liquids or dispersions of hard colloids, through fast quenching processes, such as rapidly cooling or osmotically compressing, low-frequency mechanical relaxations become increasingly slow and are accompanied by dynamic heterogeneity in the motion of the constituent molecules [2–7]. The various possible origins of dynamic heterogeneity in different types of glassy materials have been hotly debated for the past three decades.

Dynamic heterogeneity has been connected to particle configurations [8,9], but it is not significantly correlated with local structural parameters such as geometrical free volume [10] and local composition [11]. Considering that dynamic heterogeneity reflects the cooperative collective motion of particles in a glass, it is conceivable that a search for a nonlocal structural parameter may provide a better correlation between dynamic heterogeneity and structures. Low-frequency quasilocalized soft modes reflect collective excitations of particles in a potential energy landscape and have been successfully used to predict dynamic heterogeneity in quenched glasses of colloidal spheres [12,13]. However, a static structural parameter is still needed in order to directly link dynamics and structure in real space. Soft spots in glasses, defined by soft modes, are found to overlap with rearranging regions in glasses [13–15], but they typically show no qualitative differences in structure when compared to the background [15]. So, finding a suitable structural parameter remains quite challenging. Several parameters, such as the bond orientational order parameter and the local structural entropy (or the two-body translational correlation contribution to the excess entropy) S_2 [16,17], have been shown to be good structural indicators for predicting dynamic heterogeneity but only in specific systems [18–20].

All of the above work has focused on quenched colloidal glasses formed by spheres or disks. By contrast, the correlation between dynamics and structures in glass systems of hard anisotropic (i.e., nonspherical or nondiskotic) colloids has remained largely unexplored. Recently, in a 2D glass system of monodisperse prolate ellipsoids, the structural signatures for both translational and rotational dynamics have been shown [21], and S_2 performed as a reasonable static structural parameter linked to dynamic heterogeneity [22]. In contrast to this quenched ellipsoid glass, Zhao and Mason observed a 2D glass in a system of monodisperse hard kite platelets formed under a quasistatic near-equilibrium manner (i.e., very slow crowding) [23]. Each Penrose kite has fore-aft asymmetry and a well-defined pointing direction, not just an axis, leading to a larger number of distinguishably different local configurations compared to ellipsoids. Moreover, in this kite glass, no local liquid crystal ordering was observed, which is very different than the nematiclike glassy clusters observed in the ellipsoid glass. Also, regarding diffusive dynamics of an isolated particle, by contrast to a highly prolate ellipsoid [24], an isolated prismatic kite in a dilute noninteracting fluid does not show obvious anisotropic translational diffusion in the plane (i.e., there is essentially no detectable difference between an isolated kite diffusing along or diffusing perpendicular to its symmetry axis [25]). In the fluid state at higher $\phi_A = 0.35$, there is still no apparent anisotropic translational diffusion. These differences raise interesting questions about which structural parameters can be used to predict dynamic heterogeneity in the kite glass. Particularly, the relative contributions of translational motion and rotational motion to the glassy dynamics, including dynamic heterogeneity, have not been previously predicted or observed for such systems containing anisotropic glass-forming shapes that have been slowly crowded.

In this Letter, we investigate the relationship between structure and dynamics in a 2D colloidal Penrose kite glass at different area fractions ϕ_A. From experimentally obtained microscopic movies of this Brownian system, we perform customized video tracking of positions and orientations of many kites in the field of view over time. Based on these experimental results, we then calculate the intrinsic vibrational modes of the kite glass at different ϕ_A using replica undamped shadow kite systems. Soft modes are found only in the rotational vibrational modes. We also report participation fractions and participation ratios as a function of frequency ω for both translational and rotational modes. Our results demonstrate a strong spatial correlation between localized vibrational structure, static structure characterized by S_2, and dynamic heterogeneity characterized by Debye-Waller factors (DWFs).

The kite glass is composed of monodisperse colloidal Penrose kites that are four-sided polygonal platelets, each having three 72° and one 144° internal angles with two long edges of 2.9 μm, two short edges of 1.8 μm, and a thickness of 1.4 μm (see Fig. S1 in Ref. [25] for a microscopic image of a kite); the methods of lithographically mass producing these kites out of a polymeric photoresist, dispersing them in an aqueous solution, and slowly crowding them in a 2D monolayer while preserving near-hard in-plane interactions using roughness-controlled depletion attractions has been previously reported [23].

To measure the vibrational characteristics of the kite glass, we employ covariance matrix techniques [26–29] to particle-tracking data that we extract from movies of dense systems of kites at different particle area fractions ϕ_A, obtained using optical microscopy. Data were collected for about 260 sec with a total of ~3200 frames, which is higher than the total number of degrees of freedom, $3N \sim 1200$ ($N \sim 400$, the number of kites in the field of view). No cage rearrangements occurred in the chosen field of view during the selected time window. From the movies, both the centers and vertices of all kites in successive video frames are determined and analyzed using user-written interactive data language routines [23]. The uncertainty in a spatial coordinate of the center of a single kite is estimated to be about ±60 nm, and the uncertainty in the orientation of a kite found by our center and vertex detection methods is about ±5° [23]. Based on these data, we define $\boldsymbol{u}(t)$ as the $3N$-component vector of displacements of N particles from their time-averaged positions and time-averaged orientations, $\boldsymbol{u}(t) = [x_k(t) - \langle x_k \rangle, y_k(t) - \langle y_k \rangle, \theta_k(t) - \langle \theta_k \rangle]$, where the index k runs from $1, ..., N$. The system's covariance matrix at time t is defined as $C_{ij}(t) = \langle u_i(t) u_j(t) \rangle$, where indices $i, j = 1, \ldots, 3N$ run over all particles and coordinates, including both the position and orientation, and $\langle\rangle$ indicates averaging over time. In the harmonic approximation, C is directly related to the stiffness matrix K by $C_{ij} = k_B T (K^{-1})_{ij}$ [26,29]. Then the dynamical matrix can be calculated as $D_{ij} = K_{ij}/m_{ij}$, where $m_{ij} = \sqrt{m_i m_j}$ and m_i is the mass (for translational degrees of freedom) or the moment of inertia (for rotational degrees of freedom) of kite i. The eigenvectors and eigenvalues of the dynamical matrix correspond to the amplitudes and frequencies of corresponding vibrational modes, respectively. The covariance method describes a "shadow" system which has the same geometric configurations and interparticle potential but without damping as in experimental colloidal systems [30].

Figure 1 shows the displacement vector of three typical eigenmodes of the kite glass ($\phi_A = 0.60$) at selected frequencies. By contrast to earlier studies on sphere [29] or ellipsoid glasses [26] in which the low-frequency eigenmodes are quasilocalized, in the kite glass, translational displacements at the selected low ω are not localized but instead exhibit wavelike [31] features. As a consequence of crowding, the rotational displacements of most kites have small magnitudes. At intermediate ω, the eigenmodes reveal an apparent, disordered displacement distributions both in translation and in rotation, indicating a mixed character of translation and rotation. At the selected high ω, both translational and rotational displacements are localized, similar to other colloidal glasses [26,29].

The obtained vibrational density of states $D(\omega)$ of the kite glass is shown in Fig. 2(a). The slope of the $D(\omega)$ curve at low frequencies decreases as ϕ_A decreases, indicating that low-ω modes increase as the system approaches to the glass transition point ϕ_g from above (i.e., $\phi_A > \phi_g$, ϕ_g is ~0.58 in the kite system [23]). Similar behavior has been reported in granular jamming [32]. For two-dimensional crystals, the asymptotic low-ω density of states obeys the Debye relation $D(\omega) \sim \omega$. By contrast, the measured $D(\omega)/\omega$ in the kite glass is not flat but has extra low-frequency vibrational modes. This is consistent to observations in other colloidal glass systems [29,33].

To further evaluate the contributions of translation and rotation to vibrational modes, the translational and rotational participation fractions P_F^{tran} and P_F^{rot}, respectively, are calculated by $P_F^{\mathrm{tran}}(\omega) = \sum_i [\boldsymbol{e}_{ix}^2(\omega) + \boldsymbol{e}_{iy}^2(\omega)]$ and $P_F^{\mathrm{rot}}(\omega) = 1 - P_F^{\mathrm{tran}}(\omega) = \sum_i \boldsymbol{e}_{i\theta}^2(\omega)$; here eigenvectors of each mode are normalized such that $\sum_i [\boldsymbol{e}_{ix}^2(\omega) + \boldsymbol{e}_{iy}^2(\omega) + \boldsymbol{e}_{i\theta}^2(\omega)] = 1$,

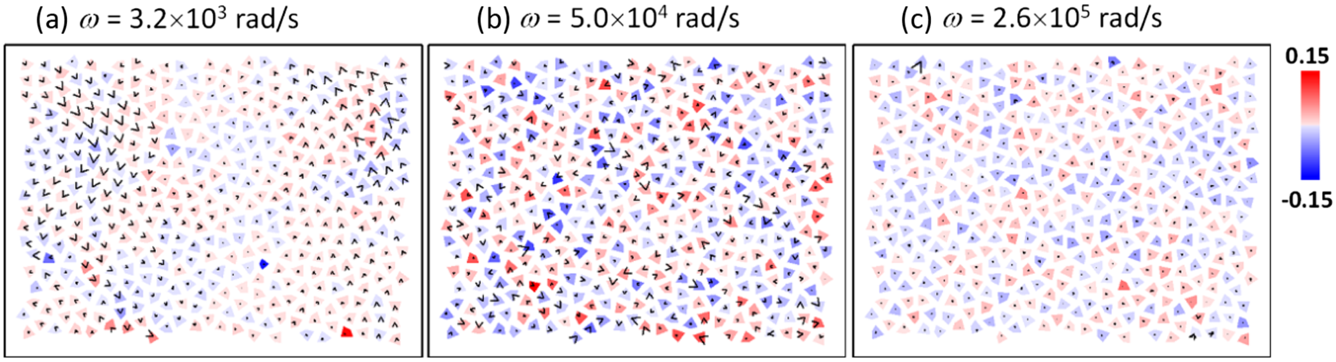

FIG. 1. Typical eigenmodes at (a) small ($\omega = 3.2 \times 10^3$ rad/s), (b) intermediate ($\omega = 5.0 \times 10^4$ rad/s), and (c) large frequencies ($\omega = 2.6 \times 10^5$ rad/s). For each particle, the pointing direction of the black arrow head shows the direction of translational displacement, and the size of the arrow head scales with the magnitude of translational displacement; the color intensity scales with the magnitude of rotational displacement (in rad) with red for counterclockwise rotation and blue for clockwise rotation.

and i runs over all particles. The results are shown in Fig. 2(c). P_F^{tran} is higher than P_F^{rot} at both low and high frequencies for all tested ϕ_A, indicating a primarily translational character at those frequencies. This observation is quite different from the results of ellipsoids, where the low-frequency regime is dominated either by rotational modes shown in a near-jammed system of ellipsoids or by a mix of translational and rotational modes shown in a glass of polydisperse ellipsoids [26,34,35]. In our kite glasses, P_F^{rot} becomes comparable to P_F^{tran} (which means a strong mixed character of translation and rotation) only in a narrow intermediate frequency range (4.6×10^4 rad/s $< \omega < 7.7 \times 10^4$ rad/s).

To characterize the degree of localization of translation and rotation in each mode, both translational and rotational participation ratios are calculated by $P_R^{\mathrm{tran}}(\omega) = \{\sum_i [\mathbf{e}_{ix}^2(\omega) + \mathbf{e}_{iy}^2(\omega)]\}^2 / \{N \sum_i [\mathbf{e}_{ix}^2(\omega) + \mathbf{e}_{iy}^2(\omega)]^2\}$ and $P_R^{\mathrm{rot}}(\omega) = [\sum_i \mathbf{e}_{i\theta}^2(\omega)]^2 / [N \sum_i \mathbf{e}_{i\theta}^4(\omega)]$. Thus, P_R^{tran}(or P_R^{rot}) $\sim 1/N$ for a strongly localized translational (or rotational) motion and P_R^{tran}(or P_R^{rot}) $\sim \mathcal{O}(1)$ for an extended motion. In glassy [26,36,37] spheres, the participation ratio (P_R) drops from ∼0.5 to below 0.2 at low frequencies. This low-ω quasilocalized character is an important feature in glass, as it is related to the spatial dynamic heterogeneity [12,38]. By contrast, in the kite glass, P_R^{tran} does not drop

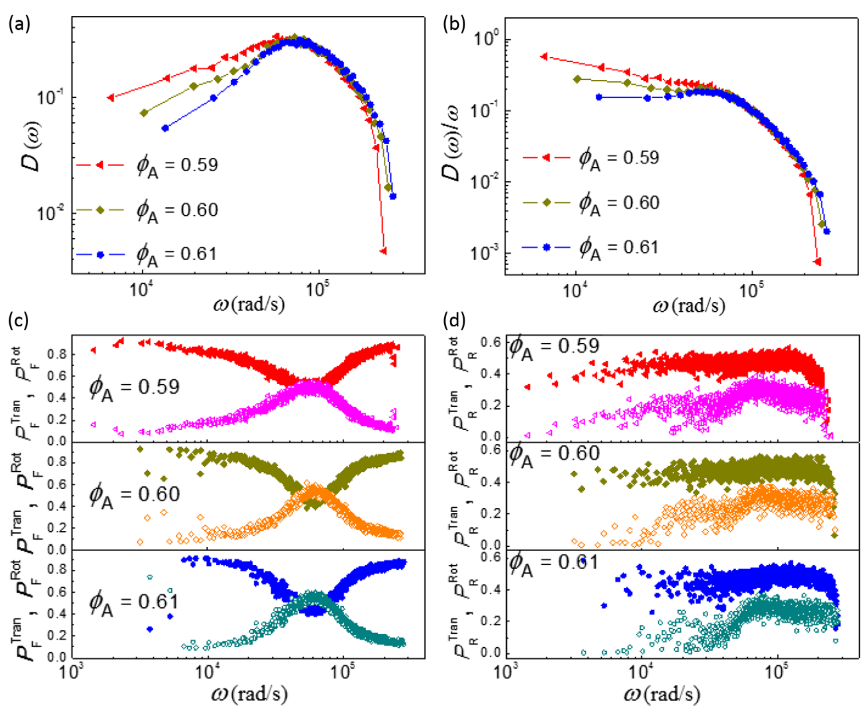

FIG. 2. (a) $D(\omega)$, (b) $D(\omega)/\omega$, (c) P_F^{tran} (solid symbol, upper curve) and P_F^{rot} (open symbol, lower curve), and (d) P_R^{tran} (solid symbol, upper curve) and P_R^{rot} (open symbol, lower curve) vs ω at different ϕ_A. (a) and (b) are bin averaged with a bin size of 30 consecutive vibrational modes.

much at low frequencies (i.e., nonlocalized) [Fig. 2(d)], which is consistent with the wavelike pattern of translational displacement of kites displayed at low ω (Fig. 1). This participation ratio difference at the low ω also agrees with the observation that the maximum values of translational non-Gaussian parameters $\alpha_2^{T,\max}$ are much smaller in the kite glass (~0.18 at $\phi_A = 0.59$; see Fig. S6E in Ref. [23]) than that in an ellipsoid glass ($\alpha_2^{\max} \sim 2$ in a glass state with volume fraction ~0.81, which just passes the glass transition point ~0.79) [21], since a lower participation ratio at low ω correlates to a spatial dynamic heterogeneity which then leads to a higher $\alpha_2^{T,\max}$. We then look for a possible structural origin for the observations by examining the local polymorphic configurations (LPCs) of kites in the glass, which was proposed in Ref. [23]. A quantitative measurement shows that each polymorph has roughly the same probability of appearance in the kite glass, although the one that can form a crystal is slightly higher (see Figs. S2–S4 in Ref. [25] for details). This suggests that in terms of excitation energy those different LPCs are more or less equivalent, so the whole system has few unique local configurations that can be differentiated from the rest of the system. This is unlike other colloidal glasses, in which dynamic heterogeneity is correlated to some local order structures (for instance, local structures having bond orientational order) in a disordered background [19,39]. In other words, the kite glass formed through the competition of those LPCs is uniformly disordered and has few structural soft spots to facilitate localized translational motion at low frequencies; thus, $\alpha_2^{T,\max}$ is small and the translational motion is not localized at low ω. The rotational motion in the kite glass, on the other hand, is localized at low ω, as indicated by small P_R^{rot} at low ω shown in Fig. 2(d). This agrees with the observation in Fig. 1 that there are only a few spotted kites with deep red or blue colors. This is also consistent with the result that the maximum value of rotational non-Gaussian parameters $\alpha_2^{R,\max}$ (~0.67 at $\phi_A = 0.59$) is larger than the corresponding $\alpha_2^{T,\max}$ (~0.18 at $\phi_A = 0.59$), which was reported in Ref. [23]. The vibrational properties of a supercooled liquid state of kites at $\phi_A = 0.57$ has also been characterized (see Fig. S5 in Ref. [25]), and the results indicate not-localized translational motion and localized rotational motion at a low frequency, similar to kites in the glass state.

The low-ω quasilocalized soft modes have been shown to be related to spatial dynamic heterogeneity in isotropic colloidal glasses [12,38]. To check this correlation in the kite glass, for rotation, we choose the low-ω modes with $P_R^{\mathrm{rot}} < 0.1$ as rotational soft modes, which includes 20 modes. For translation, because translation in the kite glass is not localized at the low-ω region, we then just choose the 20 lowest-frequency modes. The translational (p_i^{tran}) and rotational (p_i^{rot}) participation fractions [26,38,40] of kite i in these chosen modes are calculated as

$$p_i^{\mathrm{tran}} = \frac{1}{N_{\mathrm{SM}}} \sum_{\mathrm{tran}_{20}} [\boldsymbol{e}_{ix}^2(\omega) + \boldsymbol{e}_{iy}^2(\omega)], \tag{1}$$

$$p_i^{\mathrm{rot}} = \frac{1}{N_{\mathrm{SM}}} \sum_{\mathrm{rot}_{\mathrm{soft}}} \boldsymbol{e}_{i\theta}^2(\omega), \tag{2}$$

where N_{SM} is the number of chosen modes. The dynamics of the kite system are characterized by DWF, which has been shown to be a good parameter for predicting both the long- and short-time dynamic heterogeneity [41]. For each kite i, both the local translational DWF (TDWF) and the local rotational DWF (RDWF) are measured, which are defined as the mean-squared deviation of a particle from its averaged position and orientation, respectively. $\mathrm{TDWF}_i = \langle(\langle\mathbf{r}_i\rangle - \mathbf{r}_i(t))^2\rangle$ and $\mathrm{RDWF}_i = \langle(\langle\theta_i\rangle - \theta_i(t))^2\rangle$, where $\mathbf{r}_i(t)$ and $\theta_i(t)$ are the position and orientation, respectively, of particle i at time t and $\langle\rangle$ refers to time averaging over a short time corresponding to the middle of the plateau region in the mean-squared (angular) displacement. The results show that the spatial patterns of chosen modes match well with the spatial distribution of local DWF in both translation and rotation (Figs. 3 and S6). Spearman's rank-order correlation coefficient [42,43] is calculated to qualitatively evaluate the correlations (see [25] for details), and the results show that the correlation is 0.88, 0.88, and 0.89 between p^{tran} and TDWF and is 0.89, 0.85, and 0.81 between p^{rot} and RDWF for samples of $\phi_A = 0.59$, 0.60, and 0.61, respectively. The high correlation values suggest that the soft mode is a good thermodynamic parameter to correlate spatially with dynamic heterogeneity.

To further search for a structural parameter that can be used to predict dynamic heterogeneity, the bond orientational order parameter $\Psi_6(\boldsymbol{r}_i) = N_i^{-1} \sum_{j=1}^{N_i} \boldsymbol{e}^{i6\theta_{ij}}$ and local orientational order parameter $\phi_2 = \sum_{j=1}^{N_i} \cos(2\Delta\theta_j)/N_i$

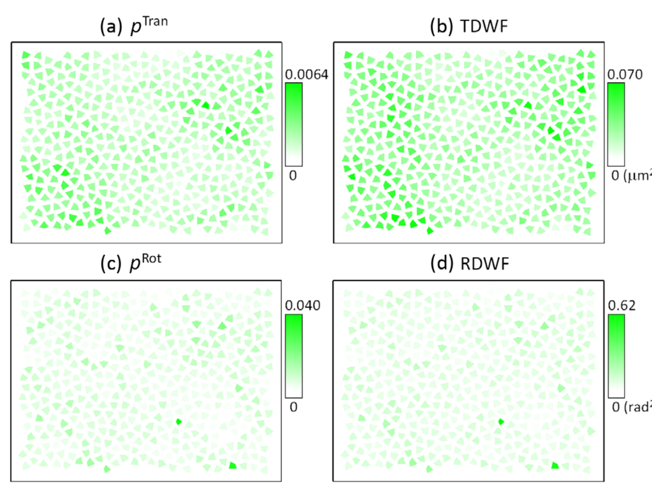

FIG. 3. Maps of kites displaying (a) p^{tran} of the 20 lowest-ω modes and (c) p^{rot} of soft modes and (b) TDWF and (d) RDWF for samples at $\phi_A = 0.60$. The color intensity scales with the amplitude of the participation fraction of chosen modes or DWFs.

[25] are tested, where N_i is the number of nearest neighbors defined by Voronoi construction of particle i, θ_{ij} is the angle between an arbitrary reference axis and the line connecting the centers of particle i and its nearest neighbor j, and $\Delta\theta_j$ is the orientational angle difference between the particle i and its nearest neighbor j. The correlation between Ψ_6 and TDWF is 0.07, 0.03, and −0.01 and that between ϕ_2 and RDWF is −0.13, −0.02, and 0.03 for samples with $\phi_A = 0.59$, 0.60, and 0.61, respectively. Both parameters show no correlation with the dynamics in the kite glass. The structural entropy S_2 measures the entropy loss due to positional or orientational correlation which can be obtained from the two-body correlation degree of the local structures. The translational and rotational S_2 of kite i are calculated, respectively, as [22,44]

$$S_{2,i}^{\mathrm{tran}} = -\pi k_B \rho \int_0^\infty [g_i(r) \ln g_i(r) - g_i(r) + 1] r dr, \quad (3)$$

$$S_{2,i}^{\mathrm{rot}} = -\frac{1}{2} k_B \rho \int_0^\infty g_i(r) r dr \int_0^{2\pi} g_i(\theta|r) \ln[g_i(\theta|r)] d\theta, \quad (4)$$

where k_B is Boltzmann's constant, ρ is the number density, $g_i(r)$ is the radial distribution function of centers of mass relative to particle i, and $g_i(\theta|r)$ is the orientational distribution function of the angular difference between the pointing direction of particle i and the particle at center-of-mass distance r. To compare with the dynamics, we overlay the particles with the top 10% largest DWF (i.e., the top 10% fastest particles) on the contour of S_2 (Figs. 4 and S7 [25]). The results show that most of the selected particles fall into the regions having high S_2 for both translation and rotation. The correlation is 0.32, 0.34, and 0.34 between S_2^{tran} and TDWF and 0.70, 0.56, and 0.47 between S_2^{rot} and RDWF for samples of $\phi_A = 0.59$, 0.60, and 0.61, respectively. So we find that S_2 exhibits a good correlation with dynamics in both translation and rotation in the kite glass, although the correlation between S_2^{tran} and TDWF is lower than that between S_2^{rot} and RDWF, which is likely due to the subtle dynamic heterogeneity associated with translation.

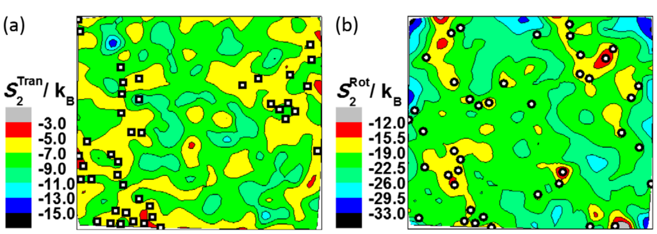

FIG. 4. Spatial distribution of S_2 and selected particles with the largest DWFs. Contour plots, (a) local S_2^{tran} and (b) local S_2^{rot}; squares, positions of selected particles (top 10% largest TDWF); and circles, positions of selected particles (top 10% largest RDWF) for $\phi_A = 0.60$.

In other glass systems, local S_2 has been shown to be linked to dynamics. Tanaka's group [18,19] simulated hard sphere glass systems and found the slow dynamics are linked to lower S_2. Zheng *et al.* [22] showed that the slow dynamics are linked to lower S_2 in both translation and rotation in a colloidal ellipsoid glass system. In those systems, however, the regions identified as domains of the dynamic heterogeneity often show a certain order such as Ψ_6 [39] or nematic order [22], although very locally. By contrast, in the kite glass, the system is frustrated by many LPCs which compete with each other. Those LPCs have different symmetries and structures, which suppress any order in the system even locally. Among the polymorphs, sixfold symmetry or orientationally aligned structures are not particularly favored. Thus, Ψ_6 and ϕ_2 show near zero correlations to local dynamics. However, S_2 seems to correlate with the dynamics in the kite glass to a substantial extent, implying a certain degree of generality of S_2 in predicting the dynamic heterogeneity in different glass systems.

In conclusion, we have examined the vibrational properties of the kite glass using covariance matrix techniques. Different from other previously investigated colloidal glasses formed by spheres or ellipsoids, in the low-ω regime, the vibrational modes of the kite glass are dominantly translational in character. The low-ω rotational modes are truly localized; however, the low-ω translational modes are extended with a crystal-level-like P_R, and the corresponding translational displacements exhibit wavelike features. One possible structural cause for the observed low-ω vibrational properties is due to the extreme diversity of incommensurate LPCs that occupy similar area fractions in the kite glass, which makes the kite glass more structurally disordered to smaller length scales, as compared to other colloidal glasses that have a significant population of locally ordered structures in a disordered background that can occur through a rapid quenching process. The pattern of the obtained soft modes (20 lowest ω modes for translation) matches well with the spatial distribution of DWFs both translationally and rotationally. Among the tested structural parameters, S_2 shows a good correlation with the distribution of particle dynamics, but Ψ_6 and ϕ_2 do not. These results indicate that such soft modes typify a near-thermodynamic structure, and the local structural entropy that characterizes a static structure is a useful parameter that is well correlated with local particle dynamics. Our findings shed new light on the origin of heterogeneous dynamics in 2D glassy systems consisting of anisotropic particles formed through slow crowding rather than rapid quenching.

We thank Xiunan Yang for thoughtful discussion. This work is supported by the National Natural Science Foundation of China (21573159 and 21621004 to K. Z., 11704276 to Y. Z. and 11474327, 11874395 to K. C.). K. C. also acknowledges support from MOST 973 Program (No. 2015CB856800). T. G. M. acknowledges financial support from UCLA.

*Corresponding author.
kunzhao@tju.edu.cn

[1] P. W. Anderson, Science **267**, 1610 (1995).
[2] W. Kob, C. Donati, S. J. Plimpton, P. H. Poole, and S. C. Glotzer, Phys. Rev. Lett. **79**, 2827 (1997).
[3] C. Donati, J. F. Douglas, W. Kob, S. J. Plimpton, P. H. Poole, and S. C. Glotzer, Phys. Rev. Lett. **80**, 2338 (1998).
[4] E. R. Weeks, J. C. Crocker, A. C. Levitt, A. Schofield, and D. A. Weitz, Science **287**, 627 (2000).
[5] G. L. Hunter and E. R. Weeks, Rep. Prog. Phys. **75**, 066501 (2012).
[6] M. D. Ediger, C. A. Angell, and S. R. Nagel, J. Phys. Chem. **100**, 13200 (1996).
[7] F. H. Stillinger and P. G. Debenedetti, Annu. Rev. Condens. Matter Phys. **4**, 263 (2013).
[8] G. C. Cianci, R. E. Courtland, and E. R. Weeks, Solid State Commun. **139**, 599 (2006).
[9] A. Widmer-Cooper, P. Harrowell, and H. Fynewever, Phys. Rev. Lett. **93**, 135701 (2004).
[10] A. Widmer-Cooper and P. Harrowell, J. Non-Cryst. Solids **352**, 5098 (2006).
[11] A. Widmer-Cooper and P. Harrowell, J. Phys. Condens. Matter **17**, S4025 (2005).
[12] M. Mosayebi, P. Ilg, A. Widmer-Cooper, and E. Del Gado, Phys. Rev. Lett. **112**, 105503 (2014).
[13] A. Widmer-Cooper, H. Perry, P. Harrowell, and D. R. Reichman, Nat. Phys. **4**, 711 (2008).
[14] K. Chen, M. L. Manning, P. J. Yunker, W. G. Ellenbroek, Z. X. Zhang, A. J. Liu, and A. G. Yodh, Phys. Rev. Lett. **107**, 108301 (2011).
[15] M. L. Manning and A. J. Liu, Phys. Rev. Lett. **107**, 108302 (2011).
[16] R. D. Mountain and H. J. Raveché, J. Chem. Phys. **55**, 2250 (1971).
[17] R. E. Nettleton and M. S. Green, J. Chem. Phys. **29**, 1365 (1958).
[18] H. Tanaka, T. Kawasaki, H. Shintani, and K. Watanabe, Nat. Mater. **9**, 324 (2010).
[19] T. Kawasaki and H. Tanaka, J. Phys. Condens. Matter **23**, 194121 (2011).
[20] T. Kawasaki, T. Araki, and H. Tanaka, Phys. Rev. Lett. **99**, 215701 (2007).
[21] Z. Y. Zheng, F. Wang, and Y. L. Han, Phys. Rev. Lett. **107**, 065702 (2011).
[22] Z. Y. Zheng, R. Ni, F. Wang, M. Dijkstra, Y. R. Wang, and Y. L. Han, Nat. Commun. **5**, 3829 (2014).
[23] K. Zhao and T. G. Mason, Proc. Natl. Acad. Sci. U.S.A. **112**, 12063 (2015).
[24] Y. Han, A. M. Alsayed, M. Nobili, J. Zhang, T. C. Lubensky, and A. G. Yodh, Science **314**, 626 (2006).
[25] See Supplemental Material at http://link.aps.org/supplemental/10.1103/PhysRevLett.121.228003 for additional experimental details, including details on the diffusive dynamics of kites in the non-interacting and in the ergodic fluid state, Spearman's rank-order correlation coefficient, the bond and local orientational order parameters, and the measurement of appearance probability of local polymorphic configurations, as well as Supplementary Figs. S1–S7.
[26] P. J. Yunker, K. Chen, Z. Zhang, W. G. Ellenbroek, A. J. Liu, and A. G. Yodh, Phys. Rev. E **83**, 011403 (2011).
[27] A. Ghosh, V. K. Chikkadi, P. Schall, J. Kurchan, and D. Bonn, Phys. Rev. Lett. **104**, 248305 (2010).
[28] D. Kaya, N. L. Green, C. E. Maloney, and M. F. Islam, Science **329**, 656 (2010).
[29] K. Chen, W. G. Ellenbroek, Z. Zhang, D. T. N. Chen, P. J. Yunker, S. Henkes, C. Brito, O. Dauchot, W. van Saarloos, A. J. Liu, and A. G. Yodh, Phys. Rev. Lett. **105**, 025501 (2010).
[30] S. Henkes, C. Brito, and O. Dauchot, Soft Matter **8**, 6092 (2012).
[31] K. Chen, T. Still, S. Schoenholz, K. B. Aptowicz, M. Schindler, A. C. Maggs, A. J. Liu, and A. G. Yodh, Phys. Rev. E **88**, 022315 (2013).
[32] L. E. Silbert, A. J. Liu, and S. R. Nagel, Phys. Rev. Lett. **95**, 098301 (2005).
[33] H. Shintani and H. Tanaka, Nat. Mater. **7**, 870 (2008).
[34] Z. Zeravcic, N. Xu, A. J. Liu, S. R. Nagel, and W. van Saarloos, Europhys. Lett. **87**, 26001 (2009).
[35] M. Mailman, C. F. Schreck, C. S. O'Hern, and B. Chakraborty, Phys. Rev. Lett. **102**, 255501 (2009).
[36] H. R. Schober and B. B. Laird, Phys. Rev. B **44**, 6746 (1991).
[37] H. Schober and G. Ruocco, Philos. Mag. **84**, 1361 (2004).
[38] A. Widmer-Cooper, H. Perry, P. Harrowell, and D. R. Reichman, J. Chem. Phys. **131**, 194508 (2009).
[39] H. Shintani and H. Tanaka, Nat. Phys. **2**, 200 (2006).
[40] D. Zhou, F. Wang, B. Li, X. J. Lou, and Y. L. Han, Phys. Rev. X **7**, 021030 (2017).
[41] A. Widmer-Cooper and P. Harrowell, Phys. Rev. Lett. **96**, 185701 (2006).
[42] X. N. Yang, R. Liu, M. C. Yang, W. H. Wang, and K. Chen, Phys. Rev. Lett. **116**, 238003 (2016).
[43] H. Tong and N. Xu, Phys. Rev. E **90**, 010401 (2014).
[44] D. Costa, F. Micali, F. Saija, and P. V. Giaquinta, J. Phys. Chem. B **106**, 12297 (2002).